BioChip J. (2012) 6(4): 396-403
DOI 10.1007/s13206-012-6412-0

Original Research

Water-stable single-walled carbon nanotubes coated by pyrenyl polyethylene glycol for fluorescence imaging and photothermal therapy

Kuewhan Jang[1], Kilho Eom[2], Gyudo Lee[2], Jae-Hee Han[3], Seungjoo Haam[4], Jaemoon Yang[5], Eunseon Kim[6], Woo-Jae Kim[6] & Taeyun Kwon[2]

Received: 30 August 2012 / Accepted: 15 October 2012 / Published online: 20 December 2012

Abstract Nanomaterials have recently received significant attention as photothermal agents and fluorescence contrast agents for molecular therapeutics due to their unique optical properties (e.g. light absorption). In particular, single-walled carbon nanotubes (SWNTs) have been recently utilized as photothermal agents (for photothermal therapy) because of the solubility of SWNTs as well as their light absorbing capability at the near-infrared region. In this work, we have developed the SWNT-based photothermal agents using pyrene-based PEGylation of SWNTs. FT-IR and/or H-NMR spectroscopies have validated the PEGylation of SWNTs, and it is shown that water-soluble SWNTs are able to generate heat under near-infrared (NIR) irradiation of 5 W/cm^2. Moreover, it is found that our pyrene-based PEGylated SWNTs exhibit the fluorescence characteristic under the excitation wavelength of 340 nm. Our study sheds light on the pyrenyl PEGylated SWNTs as photothermal agents and/or fluorescence contrast agents for the future applications in molecular therapeutics.

Keywords: Single-walled carbon nanotube, Pyrenyl group, Polyethylene glycol, Fluorescence imaging agent, Photothermal therapy

[1]Department of Mechanical Engineering, Korea University, Seoul 136-701, Korea
[2]Department of Biomedical Engineering, Yonsei University, Wonju 220-710, Korea
[3]Department of Energy IT, Gachon University, Seongnam, Gyeonggi-do 461-701, Korea
[4]Department of Chemical Engineering and Biomolecular Engineering, Yonsei University, Seoul 120-751, Korea
[5]Department of Radiology, College of Medicine, Yonsei University, Seoul 120-752, Korea
[6]Department of Chemical and Environmental Engineering, Gachon University, Seongnam, Gyeonggi-do 461-701, Korea
Correspondence and requests for materials should be addressed to T. Kwon (✉tkwon@yonsei.ac.kr) and W.-J. Kim (✉wjkim@gachon.ac.kr)

Introduction

There has been a dramatic increase of interest in novel nanomaterial for cancer therapy in order to resolve the undesired ineffectiveness of conventional cancer therapy agents. These materials include nanoshells[1-4], gold nanorods[5-7], gold nanoparticles[8] and carbon nanotubes[4,9-11]. These nanomaterials have advantages of small size of <200 nm which is smaller than tumor pore cutoff size[12], tunable optical properties by controlling the size and shape[7,13], and ability to change surface chemistry for the tumor selectivity for enhanced cancer therapy applications[14].

For photothermal therapy, the tumor cell is destroyed by the light absorption of the nanomaterial agent causing sudden generation of heat[9]. As the result, the heat generated by nanomaterial increase the temperature, resulting in denaturation of intracellular organized biomolecules, and consequently, tumor ablation. Photothermal therapeutic agents are designed to possess strong absorption at a specific wavelength. Most photothermal agents can absorb the energy of light with wavelength of the near-infrared (NIR) region from 900 nm to 1400 nm in order to minimize the adsorption by water and to enhance the adjacent healthy tis-

sue transmissibility[15].

Among several photothermal agents, single-walled carbon nanotube (SWNT) holds particular interest due to its unique optical properties and biological applications. Specifically, SWNTs have strong light absorption at the NIR region and also semiconducting SWNTs exhibits the characteristics of photoluminescence in the NIR region[16]. Moreover, SWNTs could reach tumor cell deeply due to controllable small size and have ability to load targeting ligands[17] and various molecules such as protein, antigen and polymer on their surface[17]. According to these uniqueness, SWNTs are reported as both photothermal and fluorescent contrast agents in biological systems[4,9-11,14], and as molecular transporters to shuttle various molecule cargoes such as drugs[18], protein[19,20] and DNA[20] into cells.

In order to utilize SWNTs as photothermal agents in biological systems, SWNTs should be water soluble. SWNTs are known to be hydrophobic and insoluble in inorganic solvents such as water[21], which indicates the limitation of SWNTs for biological applications. However, by modifying the surface of SWNTs, SWNTs are able to be soluble in inorganic solvents. For example, various surfactants such as sodium dodecyl sulfate (SDS)[22] and sodium cholate (SC)[23] and various polymers[24] have been used to solubilize SWNTs in inorganic solvents. The another issue is the biocompatibility of SWNTs for their application in therapy. The biological incompatibility of SWNTs is ascribed to their toxicity[25]. PEGylated SWNTs are suggested as one of methods to solve toxicity issue and to increase biocompatibility at the same time. In particular, PEGylated SWNTs are found to have prolonged blood circulation half-life with reduced reticuloendothelial system (RES) uptake, allowing SWNTs to repeatedly pass through tumor vasculatures and to achieve the effective tumor targeting[14]. Thus well-functionalized SWNTs are promising nanomaterials for the photothermal therapeutic agents.

Many works have used phospholipids as a linker for functionalization of SWNTs with polyethyleneglycol (PEG) due to the strong adsorption of phospholipids to the sidewalls of SWNTs[4,9,14,26]. Not only that, as a linker for functionalization of SWNTs with PEG molecules, use of a pyrenyl group has also been reported[27,28]. The pyrenyl group has been known to interact strongly with the sidewalls of SWNTs by the π-stacking, a similar manner of pyrenyl group stacking to the basal plane of graphite[29]. Moreover, a previous work[30] reported pyrenyl PEG as an amphiphilic fluorescent surfactant and showed pyrenyl PEGylated SWNTs as fluorescence imaging. However, for the use of PEGylated SWNTs as photothermal therapies, previous works only used phospholipids as the linker and these PEGylated SWNTs that should require additional dyes for the bimodal applications such as fluorescence imaging[9] and MR (magnetic resonance) imaging[14]. Use of pyrenyl group as the linker can allow us to obtain fluorescence imaging with no dyes and labels. Therefore, the utilization of pyrenyl group as the linker for PEGylation will be beneficial to develop SWNT-based photothermal agent that is water-soluble and fluorescence agent at the same time.

In this paper, we investigate the SWNTs as the photothermal agents under n-IR laser irradiation and fluorescence contrast agents. We, for the first time, synthesized water-soluble and highly biocompatible SWNTs by conjugating pyrene modified polyethylene glycol (Py-PEG) to SWNTs based on π-stacking between pyrenyl group and the side wall of SWNTs. Conjugation of SWNTs was confirmed by H-NMR, FT-IR, optical absorbance spectrum and TGA analysis. Also the density of conjugated SWNTs was measured by TGA analysis. It is shown that the Py-PEG functionalized SWNTs (Py-PEG-SWNTs) were well-dispersed in deionized water, which validates the great water solubility of Py-PEG-SWNT. The Py-PEG-SWNTs complex possesses high optical absorbance in the 700 nm to 1000 nm NIR region that is transparent to biological systems and sufficient to induced heat generation in order to ablate the tumor cell under 5 W/cm^2 and the excitation wavelength of 808 nm. In addition, the Py-PEG-SWNTs complex exhibits the high fluorescence intensity at the wavelength of 382 nm and 395 nm under the excitation wavelength of 340 nm due to the fluorescence characteristics of pyrenyl groups of Py-PEG-SWNTs.

Results and Discussion

Dispersed SWNTs by chemical functionalization

Water soluble biocompatible SWNTs solution was prepared by π-stacking of pyrenyl group of Py-PEG to the side wall of SWNTs (Figure 1). We synthesized Py-PEG by coupling of 1-pyrenebutyric acid and polyethylene glycol (PEG) by an esterification process. DCC was used to prepare active carboxylate from 1-pyrenebutyric acid. Then, DMAP was used as nucleophilic catalyst to couple with prepared carboxylate through the labile ion pair between the carboxylate and the acetylpyridinium ions. Finally, the hydroxyl group of PEG and acetyl group formed an ester bond. The product was confirmed by FT-IR spectrum and H-NMR spectrum. The ester group of Py-PEG was confirmed at 1737 cm^{-1} and the peaks at 1690 cm^{-1} (marked with asterisk) that representing carboxyl group of 1-pyrenebutyric acid was no longer observed

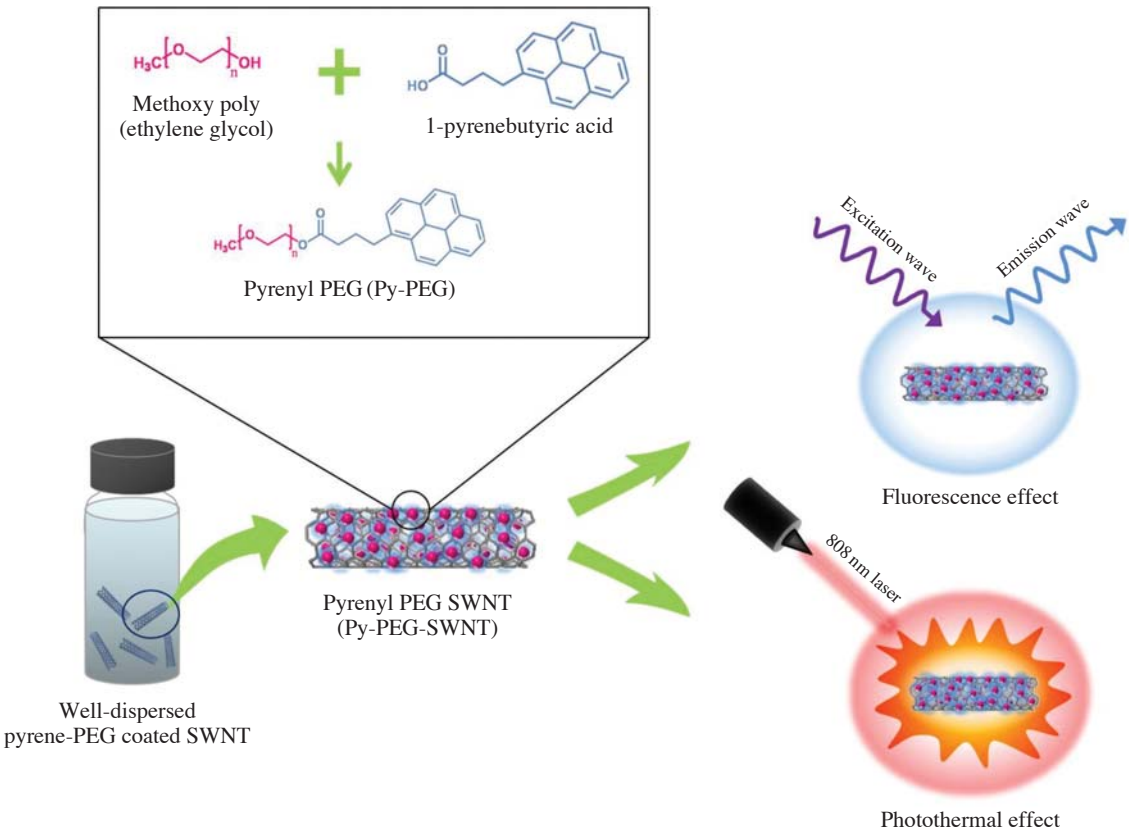

Figure 1. Schematic illustration of experimental design and chemical modification of carbon nanomaterial.

(Figure 2(a)). Moreover, H-NMR spectrum was conducted to further confirm the synthesis of Py-PEG. The H-NMR spectrum peaks between 7.95 ppm and 8.43 ppm of -CH- from 1-pyrenebutyric acid and a peak at 3.68 ppm of -CH_2- in the PEG chain were observed for the Py-PEG complex (Figure 2(b)).

To prepare Py-PEG-SWNTs, SWNTs were dissolved in Py-PEG using deionized water with vortex mixer was used to mix the solution for 24 hours. After the process, we observed the large amount of black suspensions in the solution, which were expected to be SWNT bundles. To eliminate this problem such as SWNT bundling, sonicator and centrifuge were used to disperse SWNTs in the solution. When the solution was bath-sonicated at 180 W for 8 hours, black colored solution with a few amounts of black suspensions was obtained, which suggests the well functionalized SWNTs (Figure 2(c), 2(d)). We believed that the pyrenyl group of Py-PEG functionalize to the side wall of SWNT by π stacking[29] while possessing high solubility in water from hydrogen bonding between the oxygen atoms of PEG and water molecules[31]. Finally, the well-dispersed Py-PEG-SWNT solution was centrifuged to remove the remaining SWNT bundles and the 40% of upper supernatant was collected. The upper supernatant was dialyzed for two days in order to remove remaining impurities.

The average size of Py-PEG-SWNTs was confirmed by dynamic light scattering (DLS) analysis. The average sizes obtained were 11 ± 0.4 nm, 43.2 ± 5.7 nm, 195.3 ± 29.8 nm, 7425.1 ± 505.1 nm, respectively. The size of Py-PEG-SWNTs was not uniform. We believe that the reason for the non-uniform size distribution is due to the collection of upper supernatant containing very small particles of impurities that might be the aggregates of unconjugated Py-PEG. TEM analysis was used to verify both the Py-PEG-SWNTs (Figure 2(e)) and the small particles (inset of Figure 2(e)). We have found Py-PEG-SWNTs with long and narrow structure of ~5 nm in diameter and ~100-700 nm in length. However, the round shaped small particles are ~100 nm in diameter. We conclude that the small particle does not correspond to Py-PEG-SWNTs due to the fact that small particle exhibits the rounded shape while SWNT possess the rod-like shape. Since the upper supernatant contains small particles of impurities, we decided to use lower supernatant in order to exclude the small particles. However, the lower super-

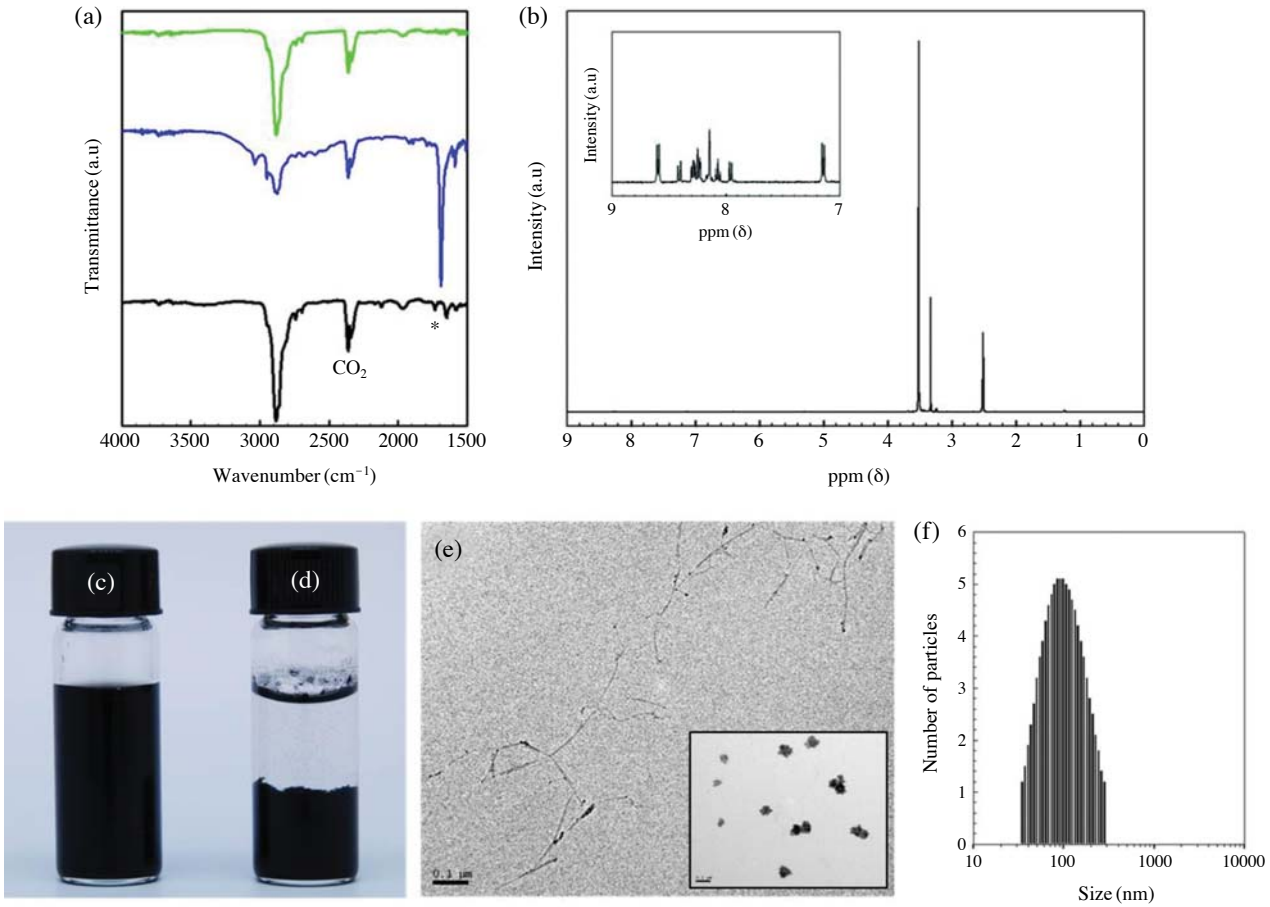

Figure 2. (a) FT-IR spectra of monomethoxy polyethylene glycol (mPEG) (green line), 1-pyrenebutyric acid (blue line), and pyrenyl PEG (Py-PEG) (black line). (b) H-NMR spectrum of Py-PEG. Photographs of glass vials containing (c) Py-PEG-SWNT and (d) bare SWNT in deionized water. (e) TEM image of Py-PEG-SWNTs. Inset: TEM image of small size particles from Py-PEG-SWNT solution. (f) DLS analysis of Py-PEG-SWNT complex in log-scale obtained from the lower supernatant with average size of 109.5 ± 56.8 nm.

natant was still expected to contain SWNTs longer than tumor pore cutoff size, therefore, 400 nm pore size syringe filter was used to obtain shorter Py-PEG-SWNTs. After the syringe filtration, the solution was dialyzed for two days and the DLS analysis was conducted. The size of particles in the solution were uniform with average size of 109.5 ± 56.8 nm (Figure 2(f)) which was smaller than the tumor pore cutoff size[12]. The FT-IR spectrum of the Py-PEG-SWNTs complex was conducted after the Py-PEG-SWNTs solution was lyophilized.

Validation of chemical functionalized SWNT

The FT-IR spectrum was obtained (Figure 3(a)) and the result showed the peak at 1737 cm^{-1} of ester bond of Py-PEG which confirms the presence of Py-PEG in Py-PEG-SWNTs complex. For further confirmation, the Py-PEG-SWNTs complex was under TGA analysis. For TGA analysis in N_2 atmosphere, 1 mL of Py-PEG-SWNTs solution (lower supernatant after centrifuge) was lyophilized and the result was obtained (Figure 3(b)). We observed the 7.1% of weight remainder even after the temperature rise of 600°C. We believe that the remaining weight is due to the SWNTs of Py-PEG-SWNTs complex because the melting temperature of pristine SWNTs and defected SWNT is 4800 K and 2600 K, respectively[32]. Because the sample was separated based on upper and lower supernatant after centrifuge, the accurate ratio of SWNT and Py-PEG in the lower supernatant cannot be estimate accurately. However, we believe that the portion of Py-PEG will be still much greater than that of SWNT in the lower supernatant because of both well-dispersed Py-PEG-SWNTs (Figure 2(e)) and the unconjugated Py-PEG residue[33]. This implies that unconjugated Py-PEG was

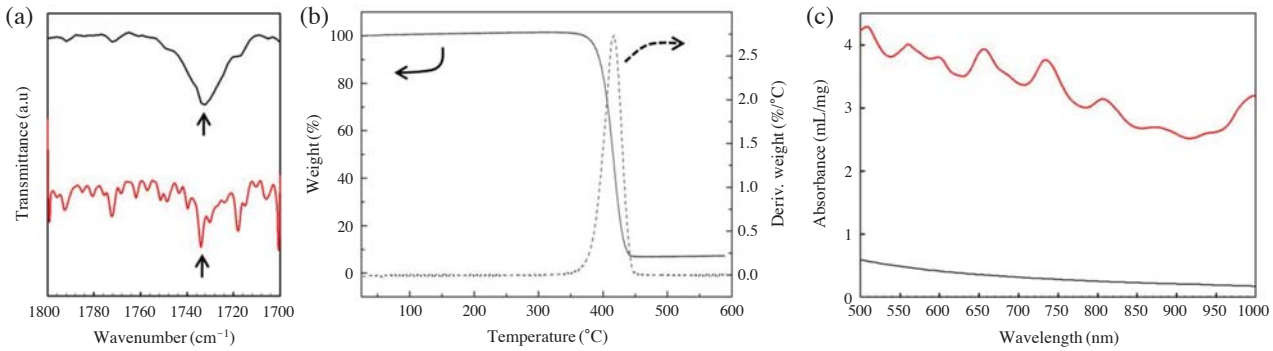

Figure 3. (a) FT-IR spectra of Py-PEG (black line) and Py-PEG-SWNT (red line) showing C=O of ester bond at 1734 cm^{-1} peak (indicated by arrow). (b) TGA result of Py-PEG-SWNT. (c) Optical absorption spectra of Py-PEG-SWNT (red line) and Py-PEG (black line) in deionized water.

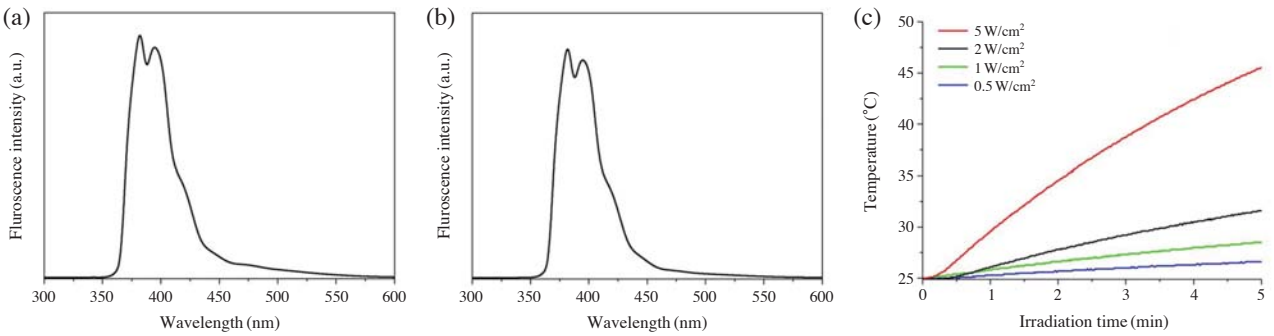

Figure 4. Fluorescence spectra of (a) Py-PEG and (b) Py-PEG-SWNT in deionized water (λ_{ex}=340 nm). (c) Temperature variation by irradiating the 808 nm wavelength laser at different irradiation power of 5 W/cm^2 (red line), 2 W/cm^2 (black line), 1 W/cm^2 (green line), and 0.5 W/cm^2 (blue line).

lyophilized with PEGylated SWNT, resulting in the increase of Py-PEG portion in TGA analysis. Moreover, it is shown that PEGylated SWNTs is ~5 nm in diameter as shown in Figure 2(e), whereas HiPco SWNTs are known to be ~0.6-1.3 nm in diameter[34]. This suggests that Py-PEG is wrapped around SWNT with ~2 nm thickness. However, because SWNT is tubular shape with one layer of carbon atoms, a portion of the mass of Py-PEG will be much greater than that of SWNT in 1 mL of the solution. In a previous study[35], a molecule dynamic (MD) simulation result of SWNT wrapped with polyethylene oxide (PEO, 3828 Da) which is similar to PEG (5000 Da) is also shown that the portion of the mass of polymer will be greater than that of SWNT as we expected[36].

Also the peak of derivative of weight was at 423°C. This result was similar to Py-PEG from control experiment (data not shown) which was at 405°C. This result suggests that decrease of weight is due to the exhaustion of Py-PEG in the Py-PEG-SWNTs complex. Finally density of SWNTs in the solution was calculated by the SWNT remainder and the density was found to be 0.857 mg/mL.

The optical absorption spectrum of Py-PEG and Py-PEG-SWNTs were obtained as shown in Figure 3(c). We have compared the optical absorbance of Py-PEG and Py-PEG-SWNTs between 700 nm to 1000 nm in the NIR region that is transparent to biological systems[15]. We observed the high optical absorbance in the NIR region with peaks but low optical absorbance of Py-PEG (Figure 3(c)). This result implies that the high optical absorbance is due to the existence of SWNTs. Those peaks of Py-PEG-SWNTs complexes were associated with the interband transition energy related with the van Hove Singularities of a quasi-1-dimensional system of SWNTs. Those interband transition energy are denoted as E_{11}, E_{22}, M_{11} etc which depends on the SWNT diameter[16]. The peaks of Py-PEG-SWNTs optical absorption spectrum were consistent with these interband transition energies. The E_{11} van hove transition of 800 nm to 1600 nm, E_{22} of 550 nm to 900 nm and M_{11} of 400 nm to 600 nm have been appeared[16]. Moreover, the well-defined peaks in the optical absorption spectrum were another signature

of well-dispersed Py-PEG-SWNTs by the functionalization of Py-PEG at the sidewall of SWNTs as expected[9].

Characterization of fluorescent and photothermal effect of Py-PEG-SWNT

The fluorescence intensity of Py-PEG and Py-PEG-SWNTs complexes were analyzed under excitation of 340 nm wavelength. Both synthesized Py-PEG and Py-PEG-SWNTs complexes exhibited high fluorescence intensity at 382 and 395 nm as shown in Figure 4(a) and 4(b). This result was similar to a previous report[30]. This result indicates that Py-PEG-SWNTs possess fluorescence properties due to Py-PEG, which suggests that Py-PEG-SWNT can play a role as the fluorescence contrast agents.

We measured the temperature change generated by 808 nm laser irradiation to examine the photothermal effect of Py-PEG-SWNTs. We controlled the irradiation powers at 0.5, 1, 2, 5 W/cm^2 for 5 minutes. The result was plotted in Figure 4(c). We observed the increase of temperature under irradiation for all the cases. However, the variation of temperatures increased as the irradiation power of laser increased. We found that 5 W/cm^2 of irradiation power reached the temperature of 46°C, which is sufficient to induce cell damage and suggests that Py-PEG-SWNT can serve as a photothermal agent[37].

Conclusions

We synthesized water-soluble SWNTs as photothermal and fluorescence contrast agents by attaching Py-PEG noncovalently to the side wall of SWNTs. The synthesized Py-PEG-SWNTs complex was water-soluble and well dispersed in deionized water. The size of Py-PEG-SWNTs complexes showed a single peak distribution with average size of 109.5 ± 56.8 nm, smaller than the tumor pore cutoff size Py-PEG-SWNTs showed the high optical absorbance in the NIR region of 700 nm to 1000 nm that is transparent to biological systems and showed the rise of temperature to 46°C sufficient to induce cell damage. Finally, Py-PEG-SWNTs exhibited high fluorescence intensity at the wavelength of 382 nm and 395 nm under the excitation wavelength of 340 nm. Our result suggests that synthesized Py-PEG-SWNTs are able to treat the tumor for future cancer therapy. However, since our work provides the preliminary results for future applications of Py-PEG-SWNT in both photothermal therapy and fluorescent imaging, the *in vitro/vivo* biomedical application such as drug delivery, the toxicity and the targetability of Py-PEG-SWNT will be considered in the future. In conclusion, Py-PEG-SWNTs complex can serve as both photothermal and fluorescence contrast agents, which paves the way for the future biomedical imaging and cancer therapy.

Materials and Methods

Materials

The following materials were purchased from Sigma Aldrich: 1-pyrenebutyric acid, 1,3-dicyclohexylcarbodiimide (DCC), 4-dimethylaminopyridine (DMAP), anhydrous dichloromethane, and triethylamine (TEA). Monomethoxy polyethylene glycol (MW: 5000 Da) was obtained from Fluka Chemical Co. HiPco SWNTs were prepared from Rice University.

Synthesis of pyrenyl polyethylene glycol (Py-PEG)

Pyrenyl polyethylene glycol (Py-PEG), an amphiphilic fluorescent surfactant, was formed by conjugating the hydroxyl group of monomethoxy polyethylene glycol (MW: 5000 Da) with the carboxyl group of 1-pyrenebutyric acid (MW: 288.34 Da) using DCC and DMAP (ref [30]). First, 1 mmol of 1-pyrenebutyric acid and 1 mmol of monomethoxy polyethylene glycol were added into a flask containing 50 mL of anhydrous dichloromethane, 9 mmol of DCC, 9 mmol of DMAP, and 9 mmol of triethylamine (Sigma Aldrich Chemical). After reacting for 48 hours at room temperature, the reactants were filtrated through a 200 nm pore size cellulose acetate filter (Advantec, CA, USA) to remove the byproduct (dicyclohexyl urea). Subsequently, the solvent was rapidly removed using a rotary evaporator (50 Hz, EYELA) and the products were washed using dichloromethane and an excess of ethyl ether. The purified precipitates were collected by vacuum filtering and lyophilized for later use.

SWNT and pyrenyl polyethylene glycol conjugation

15 mg of HiPco SWNTs and 300 mg pyrenyl polyethylene glycol (Py-PEG) were mixed in a flask containing 15 mL of deionized water. The solution were sonicated for 8 hours and centrifuged at 22,000 g for 6 hours. The 6 mL of upper supernatant and 9 mL of lower supernatant were collected separately. In case of lower supernatant, the sample was filtered using 400 nm pore size syringe filter in order to remove bundles and 2.4 mL of solution was obtained after syringe filtration. After that, both supernatants were added to 15,000 weight cut off capillary dialysis separately in a period of two days to remove remaining impurities.

808 nm laser irradiation

For photothermal studies with NIR laser irradiation, 320 μL of solution was prepared in glass vials. Prior to the laser irradiation, the samples were kept at room temperature at least 30 minutes to set the uniform initial temperature of samples. Temperature elevation of solution irradiated by NIR laser was measured through next step. The sample vial enclosed with Styrofoam vial rack was irradiated with 808 nm diode laser (JOLD-30-FC-12, JENOPTIK) with 10 mm of beam diameter for 3 minutes at power density of 0.25, 0.5, 1 and 2 W/cm^2, respectively. The Styrofoam vial racks were used as insulator for accurate measurement of temperature elevation. The elevation of temperature was measured using thermocouple (True RMS Multimeter 287, Fluke).

Characterization

The chemical structure of 1-pyrenbutyric acid, monomethoxy polyethylene glycol and pyrenyl polyethylene glycol was confirmed by an H-NMR spectrometer (Bruker DMX 400 spectrometer) with using dimethyl sulfoxide (DMSO)-d as solvent. The characteristic band of 1-pyrenbutyric acid, monomethoxy polyethylene glycol, pyrenyl polyethylene glycol and pyrenyl polyethylene glycol-SWNT complex were analyzed by Fourier-transform infrared spectroscopy (Excalibur^{TM} series, Varian) and the size distributions of those samples were measured by dynamic light scattering (ELS-Z, Otsuka electronics, Japan). The absorbance of Py-PEG-SWNTs was measured using an UV-vis spectrometer (Optizen 2120UV, MECASYS Co.). The morphologies of Py-PEG-SWNTs were evaluated by transmission electron microscope (TEM) (HR-TEM, JEM-2100 LAB6, JEOL Ltd) and the thermal properties of Py-PEG-SWNTs were measured by thermogravimetric analyzer (SDT-Q600, TA instrument).

Acknowledgements This work was supported by National Research Foundation of Korea (NRF) grant funded by the Korea government (MEST) (NRF-2010-0009428 and 2012R1A2A2A04047240) and the Human Resources Development program (No. 20104010100510) of the Korea Institute of Energy Technology Evaluation and Planning (KETEP) grant funded by the Korea government Ministry of Knowledge Economy.

References

1. Gobin, A.M. *et al*. Near-infrared resonant nanoshells for combined optical imaging and photothermal cancer therapy. *Nano Lett*. **7**, 1929-1934 (2007).
2. Hirsch, L.R. *et al*. Nanoshell-mediated near-infrared thermal therapy of tumors under magnetic resonance guidance. *Proc. Natl. Acad. Sci. USA* **100**, 13549-13554 (2003).
3. Ji, X. *et al*. Bifunctional gold nanoshells with a superparamagnetic iron oxide-silica core suitable for both MR imaging and photothermal therapy. *J. Phys. Chem. C* **111**, 6245-6251 (2007).
4. Moon, H.K., Lee, S.H. & Choi, H.C. In vivo near-infrared mediated tumor destruction by photothermal effect of carbon nanotubes. *ACS Nano* **3**, 3707-3713 (2009).
5. Choi, R. *et al*. Thiolated dextran-coated gold nanorods for photothermal ablation of inflammatory macrophages. *Langmuir* **26**, 17520-17527 (2010).
6. Dickerson, E.B. *et al*. Gold nanorod assisted near-infrared plasmonic photothermal therapy (PPTT) of squamous cell carcinoma in mice. *Cancer Lett*. **269**, 57-66 (2008).
7. Huang, X., El-Sayed, I.H., Qian, W. & El-Sayed, M.A. Cancer cell imaging and photothermal therapy in the near-infrared region by using gold nanorods. *J. Am. Chem. Soc*. **128**, 2115-2120 (2006).
8. James, F.H. *et al*. The use of gold nanoparticles to enhance radiotherapy in mice. *Phys. Med. Biol*. **49**, N309 (2004).
9. Kam, N.W.S., O'Connell, M., Wisdom, J.A. & Dai, H. Carbon nanotubes as multifunctional biological transporters and near-infrared agents for selective cancer cell destruction. *Proc. Natl. Acad. Sci. USA* **102**, 11600-11605 (2005).
10. Liu, X. *et al*. Optimization of surface chemistry on single-walled carbon nanotubes for in vivo photothermal ablation of tumors. *Biomaterials* **32**, 144-151 (2011).
11. Robinson, J. *et al*. High performance in vivo near-IR (>1 μm) imaging and photothermal cancer therapy with carbon nanotubes. *Nano Res*. **3**, 779-793 (2010).
12. Hobbs, S.K. *et al*. Regulation of transport pathways in tumor vessels: Role of tumor type and microenvironment. *Proc. Natl. Acad. Sci. USA* **95**, 4607-4612 (1998).
13. Jain, P.K. & El-Sayed, M.A. Universal scaling of plasmon coupling in metal nanostructures: extension from particle pairs to nanoshells. *Nano Lett*. **7**, 2854-2858 (2007).
14. Liu, Z. *et al*. In vivo biodistribution and highly efficient tumour targeting of carbon nanotubes in mice. *Nat. Nanotechnol*. **2**, 47-52 (2007).
15. Weissleder, R. A clearer vision for in vivo imaging. *Nat. Biotech*. **19**, 316-317 (2001).
16. O'Connell, M.J. *et al*. Band gap fluorescence from individual single-walled carbon nanotubes. *Science* **297**, 593-596 (2002).
17. Bianco, A., Kostarelos, K., Partidos, C.D. & Prato, M. Biomedical applications of functionalised carbon nanotubes. *Chem. Commun*. 571-577 (2005).
18. Bianco, A., Kostarelos, K. & Prato, M. Applications of carbon nanotubes in drug delivery. *Curr. Opin. Chem.*

Biol. **9**, 674-679 (2005).
19. Kam, N.W.S. & Dai, H. Carbon nanotubes as intracellular protein transporters: generality and biological functionality. *J. Am. Chem. Soc*. **127**, 6021-6026 (2005).
20. Kam, N.W.S., Liu, Z. & Dai, H. Carbon nanotubes as intracellular transporters for proteins and DNA: an investigation of the uptake mechanism and pathway. *Angew. Chem*. **118**, 591-595 (2006).
21. Chen, J. *et al*. Solution properties of single-walled carbon nanotubes. *Science* **282**, 95-98 (1998).
22. Moore, V.C. *et al*. Individually suspended single-walled carbon nanotubes in various surfactants. *Nano Lett*. **3**, 1379-1382 (2003).
23. Barone, P.W., Baik, S., Heller, D.A. & Strano, M.S. Near-infrared optical sensors based on single-walled carbon nanotubes. *Nat. Mater*. **4**, 86-92 (2005).
24. Nish, A., Hwang, J.-Y., Doig, J. & Nicholas, R.J. Highly selective dispersion of single-walled carbon nanotubes using aromatic polymers. *Nat. Nano*. **2**, 640-646 (2007).
25. Nel, A., Xia, T., Mädler, L. & Li, N. Toxic potential of materials at the nanolevel. *Science* **311**, 622-627 (2006).
26. Welsher, K. *et al*. A route to brightly fluorescent carbon nanotubes for near-infrared imaging in mice. *Nat. Nano*. **4**, 773-780 (2009).
27. Chen, R.J., Zhang, Y., Wang, D. & Dai, H. Noncovalent sidewall functionalization of single-walled carbon nanotubes for protein immobilization. *J. Am. Chem. Soc*. **123**, 3838-3839 (2001).
28. Prencipe, G. *et al*. PEG branched polymer for functionalization of nanomaterials with ultralong blood circulation. *J. Am. Chem. Soc*. **131**, 4783-4787 (2009).
29. Jaegfeldt, H., Kuwana, T. & Johansson, G. Electrochemical stability of catechols with a pyrene side chain strongly adsorbed on graphite electrodes for catalytic oxidation of dihydronicotinamide adenine dinucleotide. *J. Am. Chem. Soc*. **105**, 1805-1814 (1983).
30. Lim, E.-K. *et al*. Self-assembled fluorescent magnetic nanoprobes for multimode-biomedical imaging. *Biomaterials* **31**, 9310-9319 (2010).
31. Jeon, S.I., Lee, J.H., Andrade, J.D. & De Gennes, P.G. Protein-surface interactions in the presence of polyethylene oxide: I. Simplified theory. *J. Colloid Interface Sci*. **142**, 149-158 (1991).
32. Kaiwang, Z. *et al*. Melting and premelting of carbon nanotubes. *Nanotechnology* **18**, 285703 (2007).
33. Meyer, F. *et al*. Poly(amino-methacrylate) as versatile agent for carbon nanotube dispersion: an experimental, theoretical and application study. *J. Mater. Chem*. **20**, 6873-6880 (2010).
34. Bachilo, S.M. *et al*. Structure-assigned optical spectra of single-walled carbon nanotubes. *Science* **298**, 2361-2366 (2002).
35. Tallury, S.S. & Pasquinelli, M.A. Molecular dynamics simulations of flexible polymer chains wrapping single-walled carbon nanotubes. *J. Phys. Chem. B* **114**, 4122-4129 (2010).
36. Rahmat, M. & Hubert, P. Carbon nanotube-polymer interactions in nanocomposites: A review. *Compos. Sci. Technol*. **72**, 72-84 (2011).
37. Dewey, W.C. Arrhenius relationships from the molecule and cell to the clinic. *Int. J. Hyperther*. **10**, 457-483 (1994).